
Fast Adaptive Test-Time Defense with Robust Features

Anurag Singh^{*,1}
anurag.singh@cispa.de

Mahalakshmi Sabanayagam^{*,2}
sabanaya@cit.tum.de

Krikamol Muandet¹
muandet@cispa.de

Debaghya Ghoshdastidar²
ghoshdas@cit.tum.de

¹ CISPA–Helmholtz Center for Information Security, Saarbrücken, Germany

² School of Computation, Information and Technology, Technical University of Munich

Abstract

Adaptive test-time defenses are used to improve the robustness of deep neural networks to adversarial examples. However, existing methods significantly increase the inference time due to additional optimization on the model parameters or the input at test time. In this work, we propose a novel adaptive test-time defense strategy that is easy to integrate with any existing (robust) training procedure without additional test-time computation. Based on the notion of robustness of features that we present, the key idea is to project the trained models to the most robust feature space, thereby reducing the vulnerability to adversarial attacks in non-robust directions. We theoretically show that the top eigenspace of the feature matrix are more robust for a generalized additive model and support our argument for a large width neural network with the Neural Tangent Kernel (NTK) equivalence. We conduct extensive experiments on CIFAR-10 and CIFAR-100 datasets for several robustness benchmarks, including the state-of-the-art methods in RobustBench, and observe that the proposed method outperforms existing adaptive test-time defenses at much lower computation costs.

1 Introduction

Despite the phenomenal success of deep learning in several challenging tasks, they are prone to vulnerabilities such as the addition of carefully crafted small imperceptible perturbations to the input data known as adversarial examples [33, 14]. While adversarial examples are semantically similar to the input data, they cause the networks to make wrong predictions with high confidence. The primary focus of the community in building models that are robust to adversarial examples is through modified training procedures. One of the most popular and promising approaches is adversarial training [22], which minimizes the maximum loss on the perturbed input samples. Extensive empirical and theoretical studies on the robustness of deep neural networks using adversarial training reveals that adversarial examples are inevitable [17, 5, 31, 35] and developing robust deployable models with safety guarantees require a huge amount of data and model complexity [25, 38, 7]. For instance, the current state-of-the-art methods [38, 15, 29] use additional one million to 100 million generated or synthetic data along with the original 50000 training samples of CIFAR-10 and CIFAR-100. Although the improvement in robust performance is convincing with this approach, there is an evident tradeoff with huge computational costs both in terms of data and model.

While the deep learning community has focused on achieving robustness through different training paradigms such as adversarial training, little attention has been on improving the robustness of pre-trained models during inference. *Adaptive test-time defenses* refer to the class of methods that

^{*}Equal contribution. This work was partly done when AS was in TU Munich

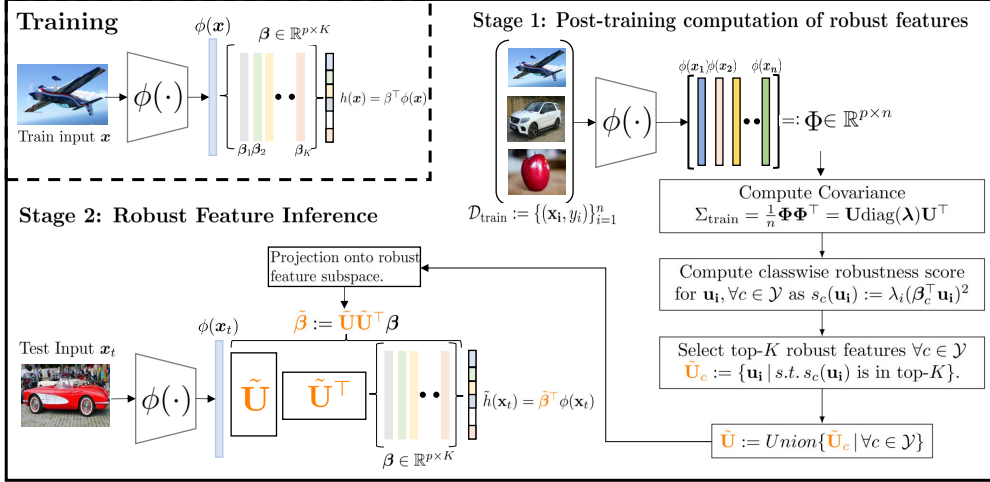


Figure 1: **Illustration of our adaptive test-time defense mechanism.** Given any trained model $h(\mathbf{x})$, we first post-process the features of the penultimate layer $\phi(\mathbf{x})$ to get the top most informative and robust features in eigenspace $\tilde{\mathbf{U}}$ using the training data. During inference of the test data \mathbf{x}_t , $\phi(\mathbf{x}_t)$ is projected onto the robust feature space using $\phi(\mathbf{x}_t) \tilde{\mathbf{U}} \tilde{\mathbf{U}}^T$, equivalently changing β to $\tilde{\beta} = \tilde{\mathbf{U}} \tilde{\mathbf{U}}^T \beta$.

improve the robustness of any trained model at test time. This is typically achieved through two main strategies, modifying the test samples before making prediction [2, 39] or updating the model parameters by adding network components like activations or new layers [19, 8]. However, inference becomes more computationally demanding because of the additional computation or data processing at test time. In fact, current state-of-the-art adaptive test-time defenses often require $40\times$ to $400\times$ additional computation at inference [39, 16, 23, 32], while not necessarily improving the robustness of the underlying model [12]. Thus, efficiently improving the adversarial robustness of the trained models at test time without additional data or model cost remains an unresolved problem.

Our contribution. In this work, we develop a novel adaptive test-time defense strategy with the *same inference cost as the underlying model* and no additional data or model complexity. In Section 3.1, we define robust features, inspired by Athalye et al. [5], Ilyas et al. [17], and subsequently describe the proposed method in Section 3.2 that relies on the idea of retaining the most robust features of the trained model. Importantly, our method is easy to integrate with any existing training paradigm. We provide a theoretical justification for our method by analyzing the robustness of features in generalized additive model setting (Corollary 2) and extend it to large width neural networks using the Neural Tangent Kernels (NTKs) equivalence [18, 4]. An interesting by-product of our analysis is a proof of the fact that robust features are learned first during standard training and that the vulnerability to adversarial examples arises from the presence of non-robust features that are learned later in the training process. This phenomenon has been observed empirically for NTK features [34] without theoretical proof. As a supplementary analysis, we prove it for NTK features (Section 3.4) and the dynamics in appendix. We conduct extensive experiments in Section 4 using different architectures such as ResNet-18, ResNet-50, WideResNet-28-10 and WideResNet-34-10 on CIFAR-10 and CIFAR-100 where our method consistently outperforms the robustness of the base models, as well as other adaptive test-time defenses. Thus, we provide the first theoretically guided method that does inference in $1\times$ time as the base model, overcoming the major criticism of the adaptive test-time defenses.

Illustration of our method (see Figure 1). The proposed method abstracts any deep neural network as a feature extractor $\phi(\mathbf{x})$ and a linear layer $\beta^T \phi(\mathbf{x})$ that consists of class prototypes. We compute the covariance of the features Σ_{train} obtained from the training examples of the feature extractor. We define a robustness measure for the eigenvectors of Σ_{train} as $s_c(\mathbf{u}_k)$ and for each class prototype, we retain only the top most eigenvectors with respect to the robustness measure. This choice of the robustness metric as well as the principle of sorting the eigenvector are mathematically justified through Corollary 2, where we consider generalized additive models and compute the robustness score of features (Definition 1) showing that the top eigenvectors of the feature matrix are more robust. For a finite-width network, the above theoretical argument essentially corresponds to projecting the

weights of only the last layer β onto the space spanned by the most robust features $\tilde{\beta} = \tilde{U}\tilde{U}^\top\beta$, thereby improving the robustness of the underlying model at test time. Our method does not increase the inference time because the selected robust eigenbasis can be used to simply transform the linear layer weights into the eigenbasis resulting in exactly the same number of parameters in the network at inference time.

2 Related Works

In recent years, there has been a significant amount of research on generating adversarial examples and simultaneously improving the robustness of deep neural networks (DNNs) against such examples. We review the most relevant works below along with adaptive test-time defenses and NTK.

Adversarial robustness. Szegedy et al. [33] first observed that the adversarial examples, which are small imperceptible perturbations to the original data, can fool the DNN easily and make incorrect predictions. To generate adversarial examples, Fast Gradient Sign Method (FGSM) is proposed by Goodfellow et al. [14]. Madry et al. [22] introduced an effective and strong defense against adversarial examples known as adversarial training, a neural network training procedure to obtain models that are robust to such examples by minimizing the maximum loss on the adversarially perturbed inputs. Adversarial training remains a promising defense strategy to significantly improve the robustness of DNNs against adversarial attacks [30, 7, 13, 38, 26]. However, sophisticated attacks are developed to break the defenses such as Carlini-Wagner (C&W) attack [6], a method for generating adversarial examples; ‘obfuscated gradients’ hypothesis [5] posits that the vulnerability to adversarial examples is due to the presence of gradients in the model that are easy to manipulate; ‘feature collision’ hypothesis [17] postulates that the vulnerability is due to the presence of features in the data that are correlated with the labels, but loses the correlation when perturbed. To counter such attacks, advanced defense strategy such as constraining the Lipschitz constant of the model [37] are developed.

Adaptive test-time defenses. Adaptive defenses are usually implemented at test time and can often change model parameters and inputs at inference, even arbitrarily, to defend against the attack. One strategy of adaptive test-time defenses is through *input purification*, which is, the inputs to a model (usually pre-trained with a robustness objective) is optimized with a test-time objective. This test-time optimization can be hand crafted [2, 39] or learned [23, 16] with the help of an auxiliary network [25, 24]. Another strategy for building adaptive test-time defenses is *model adaptation*, where model parameters are often augmented with activations [8], implicit representations [19, 28] and additional normalization layers [36]. Although several methods are developed for adaptive test-time defenses, all of them increase the inference cost atleast $2\times$ [19] and sometimes $500\times$ [32] compared to the underlying model. Furthermore, some methods are not really robust and are not competitive with the static model counterpart. Refer to Croce et al. [12] for detailed evaluation.

Adversarial attacks using Neural Tangent Kernels (NTKs). Jacot et al. [18], Arora et al. [4], Yang [40] show the equivalence of training a large width neural network by gradient descent to a deterministic kernel machine called Neural Tangent Kernel. In the context of adversarial attacks and robustness, [34] propose a method to generate adversarial examples using NTK and show transferability of the attack to the finite width neural network counterpart successfully. Additionally, the authors define NTK features using the eigenspectrum of the NTK gram matrix and observe that the robust features correspond to the top of the eigenspectrum. As a supplementary result of our analysis, we theoretically show that the robust NTK features are at the top of the spectrum and also give exact relationships in closed form for their convergence during training.

3 Adaptive Test-Time Defense Using Robust Features

We are primarily interested in the multi-class classification problem, that is, we aim to learn a predictor $h : \mathcal{X} \rightarrow \mathcal{Y}$ where $\mathcal{X} \subseteq \mathbb{R}^d$ and $\mathcal{Y} \subset \{0, 1\}^C$ is the set of one-hot encodings of C classes. We assume that the data is independent and identically distributed (i.i.d) according to an unknown joint distribution \mathcal{D} over instance-labels $(\mathbf{x}, y) \in \mathcal{X} \times \mathcal{Y}$. The goal of the paper is to develop an adaptive test-time defense mechanism that can be integrated with any existing training procedure. Hence, we assume that there exists a learned predictor $h : \mathcal{X} \rightarrow \mathcal{Y}$ that we aim to make robust against adversarial attacks. We aim to achieve this by decomposing the predictor into two components,

$h(\mathbf{x}) = h_{\text{robust}}(\mathbf{x}) + h_{\text{nonrobust}}(\mathbf{x})$ such that $h_{\text{robust}} : \mathcal{X} \rightarrow \mathcal{Y}$ corresponds to the robust component of the predictor while $h_{\text{nonrobust}} : \mathcal{X} \rightarrow \mathcal{Y}$ represents the remaining (non robust) component of h . In this section, we formally characterize this problem by proposing a notion of robustness of features, inspired by Ilyas et al. [17], and use this notion to present an algorithm in Section 3.2, based on pruning less robust features. We also show that the more robust features are more informative in Section 3.3. As a supplementary result we show that the robust NTK features correspond to the top spectrum in Section 3.4.

3.1 Robust and Non-Robust Features

The additive decomposition of a predictor in the form $h = h_{\text{robust}} + h_{\text{nonrobust}}$ is difficult in general for predictors with non-linearities in the output, for instance, softmax in multi-class classifiers. Hence, we relax the setup to a multivariate regression problem, that is, $\mathcal{Y} = \mathbb{R}^C$. We further assume that the trained model $h : \mathcal{X} \rightarrow \mathcal{Y}$ is given by a generalized additive model (GAM) of the form $h(\mathbf{x}) = \beta^\top \phi(\mathbf{x})$, where $\phi : \mathcal{X} \rightarrow \mathcal{H}$ is a smooth function that maps the data into a *feature space* \mathcal{H} and β are weights learned in the feature space. The above form of h may represent the solution of kernel regression (with \mathcal{H} being the corresponding reproducing kernel Hilbert space) or h could be the output layer of a neural network, where $\mathcal{H} = \mathbb{R}^p$, $\phi(\mathbf{x})$ denotes the representation learned in the last hidden layer and $\beta \in \mathbb{R}^{p \times C}$ are learned weights of the output layer.

Features and their robustness. To identify the robust component of h , we aim to approximate ϕ as sum of K robust components $(\phi_i)_{i=1}^K$, or alternatively, $h(\mathbf{x}) \approx \sum_{i=1}^K \beta^\top \phi_i(\mathbf{x})$. We refer to each $\phi_i : \mathcal{X} \rightarrow \mathcal{H}$ as a *feature*. More generally, we define the set of all features as $\mathcal{F} = \{f : \mathcal{X} \rightarrow \mathcal{H}\}$. We now define the robustness of a feature as follows.

Definition 1 (ℓ_2 -Robustness of features). *Given a distribution \mathcal{D} on $\mathcal{X} \times \mathbb{R}^C$ and a trained model $h(\mathbf{x}) = \beta^\top \phi(\mathbf{x})$, we define the robustness of a feature $f \in \mathcal{F}$ as $s_{\mathcal{D}, \beta}(f) = \mathbb{E}_{(\mathbf{x}, y) \sim \mathcal{D}} \left[\inf_{\|\tilde{\mathbf{x}} - \mathbf{x}\|_2 \leq \Delta} y^\top \beta^\top f(\tilde{\mathbf{x}}) \right]$, while we use $s_{\mathcal{D}, \beta, c}(f) = \mathbb{E}_{(\mathbf{x}, y) \sim \mathcal{D}} \left[\inf_{\|\tilde{\mathbf{x}} - \mathbf{x}\|_2 \leq \Delta} y_c \beta_c^\top f(\tilde{\mathbf{x}}) \right]$ to specify the robustness of f with respect to the c -th class component of $y \in \mathbb{R}^C$, where $c \in \{1, \dots, C\}$ and β_c is c -th column of β .*

The above definition is based on the notion of robust features introduced by Ilyas et al. [17], specialized to the case of GAM model. Based on Definition 1, the goal would be to approximate h using the most robust feature (or features). However, searching over all $f \in \mathcal{F}$ is difficult, and hence, we focus on features that are linear transformations of ϕ , that is, $f(x) = \mathbf{M}^\top \phi(x)$ for some $\mathbf{M} : \mathcal{H} \rightarrow \mathcal{H}$ (or in $\mathbf{M} \in \mathbb{R}^{p \times p}$). For such features, one can bound the robustness score from below, under an independent noise model.

Theorem 1 (Lower bound on robustness). *Given $h(\mathbf{x}) = \beta^\top \phi(\mathbf{x})$. Assume that the distribution \mathcal{D} is such that $y = h(\mathbf{x}) + \epsilon$, where $\epsilon \in \mathbb{R}^C$ has independent coordinates, each satisfying $\mathbb{E}[\epsilon_c] = 0$, $\mathbb{E}[\epsilon_c^2] \leq \sigma^2$ for all $c \in \{1, \dots, C\}$. Further, assume that the map ϕ is L -Lipschitz, that is, $\|\phi(\mathbf{x}) - \phi(\tilde{\mathbf{x}})\|_{\mathcal{H}} \leq L\|\mathbf{x} - \tilde{\mathbf{x}}\|$. Then, for any $f = \mathbf{M}\phi$ and every $c \in \{1, \dots, C\}$,*

$$s_{\mathcal{D}, \beta, c}(f) \geq \beta_c^\top \Sigma \mathbf{M} \beta_c - L \Delta \|\mathbf{M}\|_{op} \|\beta_c\|_{\mathcal{H}} \sqrt{\sigma^2 + \beta_c^\top \Sigma \beta_c},$$

where $\Sigma = \mathbb{E}_{\mathbf{x}} [\phi(\mathbf{x})\phi(\mathbf{x})^\top]$ and $\|\mathbf{M}\|_{op}$ denotes the operator norm.

Remark 1 (Lower bound is reasonably tight). *In the case of linear models $\phi(\mathbf{x}) = \mathbf{x}$ and assuming $\mathbb{E}_{\mathbf{x}}[\mathbf{x}] = 0$, one can compute $s_{\mathcal{D}, \beta, c}(f) = \beta_c^\top \Sigma \mathbf{M} \beta_c - \sqrt{2/\pi} \Delta \|\mathbf{M}\|_{op} \|\beta_c\|_{\mathcal{H}} \sqrt{\sigma^2 + \beta_c^\top \Sigma \beta_c}$. In this case, the lower bound in Theorem 1 is reasonably tight, differing by a constant factor of $\sqrt{2/\pi}$.*

Theorem 1 suggests that if we search only over $f \in \mathcal{F}$ that are linear transformations $f = \mathbf{M}^\top \phi$ such that $\|\mathbf{M}\|_{op} = 1$, then the most robust feature is the one that maximizes the first term $\beta_c^\top \Sigma \mathbf{M} \beta_c$. In particular, we restrict our search to projections onto K dimensional subspace, $\mathbf{M} = \mathbf{P}\mathbf{P}^\top$, where \mathbf{P} is the orthonormal basis for the subspace. We show that optimising over such features f corresponds to projecting onto top K eigenvectors \mathbf{u} of Σ sorted according to a specific *robustness score*.

Algorithm 1 Robust Feature Inference (RFI)

Require: The model h trained on $\mathcal{D}_{\text{train}} := \{(\mathbf{x}_i, y_i)\}_{i=1}^n$ such that $h(\mathbf{x}) = \boldsymbol{\beta}^\top \phi(\mathbf{x})$ where $\phi : \mathcal{X} \rightarrow \mathbb{R}^p$ and $\boldsymbol{\beta} \in \mathbb{R}^{p \times C}$, and the number of top robust features to select K .

- 1: Compute the covariance $\Sigma_{\text{train}} \leftarrow \frac{1}{n} \Phi \Phi^\top$ where $\Phi := [\phi(x_1), \dots, \phi(x_n)] \in \mathbb{R}^{p \times n}$.
- 2: Compute eigendecomposition of $\Sigma_{\text{train}} = \mathbf{U} \text{diag}(\boldsymbol{\lambda}) \mathbf{U}^\top$ where columns of \mathbf{U} are $\mathbf{u}_i \in \mathbb{R}^p$.
- 3: Select top K most robust features $\tilde{\mathbf{U}} \in \mathbb{R}^{p \times K}$ (steps 4 \rightarrow 8)
- 4: $\tilde{\mathbf{U}} \leftarrow \{\}, \boldsymbol{\beta}_c \leftarrow c$ -th column of $\boldsymbol{\beta}$
- 5: **for** $c \leftarrow 1$ to C **do**
- 6: For all i , compute robustness score $s_c(\mathbf{u}_i) \leftarrow \lambda_i (\boldsymbol{\beta}_c^\top \mathbf{u}_i)^2$
- 7: $\tilde{\mathbf{U}} \leftarrow \text{Union}(\tilde{\mathbf{U}}, \mathbf{u}_i)$ if $s_c(\mathbf{u}_i)$ is in top K scores $s_c(\cdot)$
- 8: **end for**
- 9: Robust Feature Inference on test set X_{test} (steps 10 \rightarrow 11)
- 10: $\tilde{\boldsymbol{\beta}} = \tilde{\mathbf{U}} \tilde{\mathbf{U}}^\top \boldsymbol{\beta}$
- 11: $\forall \mathbf{x}_t \in X_{\text{test}}, \tilde{h}(\mathbf{x}_t) = \tilde{\boldsymbol{\beta}}^\top \phi(\mathbf{x}_t)$

Corollary 2. Fix any K and $(\lambda_i, \mathbf{u}_i)_{i=1,2,\dots}$ denote the eigenpairs of $\Sigma = \mathbb{E}_{\mathbf{x}} [\phi(\mathbf{x})\phi(\mathbf{x})^\top]$. Consider the problem of maximizing the lower bound in Theorem 1 over all features $f \in \mathcal{F}$ that correspond to projection of ϕ onto K dimensional subspace. Then the solution is given by $f = \tilde{\mathbf{U}} \tilde{\mathbf{U}}^\top \phi$, where $\tilde{\mathbf{U}}$ is the matrix of the K eigenvectors for which the robustness score $s_c(\mathbf{u}_i) = \lambda_i (\boldsymbol{\beta}_c^\top \mathbf{u}_i)^2$ are largest.

The above results leads to principle idea of our adaptive test-time defense algorithm. The method retains and leverages only robust features of the pre-trained model at test time by effectively projecting the output of the pre-trained model to the eigenspace with higher robustness score. One may naturally ask how much error is incurred by retaining only the robust features. Later, in Section 3.3, we discuss that the most robust features also contain most of the information, and hence, drop in performance due to the projection is low.

3.2 Our Algorithm: Robust Feature Inference (RFI)

Let $\mathcal{D}_{\text{train}} := \{(\mathbf{x}_i, y_i)\}_{i=1}^n \subset \mathcal{X} \times \mathcal{Y}$ be a training dataset with n samples, and $h : \mathcal{X} \rightarrow \mathcal{Y}$ a pre-trained model such that $h(\mathbf{x}) = \boldsymbol{\beta}^\top \phi(\mathbf{x})$ for all $\mathbf{x} \in \mathcal{X}$ where $\phi : \mathcal{X} \rightarrow \mathbb{R}^p$ is the feature map defined by the hidden layers of the model h and $\boldsymbol{\beta} \in \mathbb{R}^{p \times C}$ is the weight matrix defined by the last fully-connected layer. Hence, p is the dimension of the feature space. As described in the previous section, we propose a method operating on the feature space of ϕ that projects the features in the robust directions, hence improving robustness by reducing the chance of attacks using the non-robust feature directions. To this end, we first compute the corresponding covariance matrix Σ_{train} of the hidden-layer features based on the input data from $\mathcal{D}_{\text{train}}$. In other words,

$$\Sigma_{\text{train}} = \frac{1}{n} \Phi \Phi^\top \quad \text{with} \quad \Phi := [\phi(\mathbf{x}_1), \dots, \phi(\mathbf{x}_n)] \in \mathbb{R}^{p \times n}. \quad (1)$$

Next, we compute the eigendecomposition of the feature covariance matrix $\Sigma_{\text{train}} = \mathbf{U} \text{diag}(\boldsymbol{\lambda}) \mathbf{U}^\top$ where $\mathbf{U} \in \mathbb{R}^{p \times p}$ is the matrix whose columns consist of eigenvectors of Σ_{train} denoted by $\mathbf{u}_i \in \mathbb{R}^p$, $\boldsymbol{\lambda} \in \mathbb{R}^p$ is a vector of corresponding eigenvalues such that $\lambda_1 \geq \lambda_2 \geq \dots$, and $\text{diag}(\boldsymbol{\lambda})$ is a diagonal matrix with eigenvalues as its diagonal entries. The idea of our algorithm is to retain only robustly useful features, i.e., top K eigenvectors, when making predictions on previously unseen data. For each class $c \in \mathcal{Y}$, we define the c -th column of $\boldsymbol{\beta}$ as $\boldsymbol{\beta}_c$ as class prototype for $c \in \mathcal{Y}$. The classwise robustness score of each feature is computed according to Definition 1, that is, $s_c(\mathbf{u}_i) := \lambda_i (\boldsymbol{\beta}_c^\top \mathbf{u}_i)^2$ where $(\lambda_i, \mathbf{u}_i)$ is the i -th pair of eigenvalue and eigenvector. We then select the top- K most robust features for each class $c \in \mathcal{Y}$ based on the robustness score denoted by $\tilde{\mathbf{U}}_c := \{\mathbf{u}_{\sigma(i)} \mid s_c(\mathbf{u}_{\sigma(i)}) \geq s_c(\mathbf{u}_{\sigma(j)}), \forall i, j \in [1, \dots, K]\}$. The global robust features for the model $\tilde{\mathbf{U}}$ is obtained as a union of the sets of classwise robust features $\tilde{\mathbf{U}}_c$. Finally, the prediction on a test data point \mathbf{x}_t is subsequently obtained as

$$\tilde{h}(\mathbf{x}_t) = \tilde{\boldsymbol{\beta}}^\top \phi(\mathbf{x}_t), \quad \tilde{\boldsymbol{\beta}} := \tilde{\mathbf{U}} \tilde{\mathbf{U}}^\top \boldsymbol{\beta}, \quad \tilde{\mathbf{U}} := \bigcup_{c \in \mathcal{Y}} \tilde{\mathbf{U}}_c, \quad (2)$$

where \cup denotes union of sets. Therefore, the new prediction is based on the updated parameters $\tilde{\beta}$ instead of the original β . It is not difficult to see that this corresponds to applying the original parameters β on the robustly useful features, i.e., $\tilde{h}(\mathbf{x}_t) = \tilde{\beta}^\top \phi(\mathbf{x}_t) = \beta^\top \tilde{\mathbf{U}} \tilde{\mathbf{U}}^\top \phi(\mathbf{x}_t) = \beta^\top \tilde{\phi}(\mathbf{x}_t)$ where $\tilde{\phi}(\mathbf{x}_t) := \tilde{\mathbf{U}} \tilde{\mathbf{U}}^\top \phi(\mathbf{x}_t)$. Algorithm 1 summarizes the proposed adaptive test-time defense.

3.3 Robustness vs information of features

The previous discussion focused only on robustness of features and projections onto the robust subspace. We show that the more robust features are also the more informative features. To this end, we consider the following notion of informative features, inspired by the usefulness property in [17].

Definition 2 (Informative features). *Given a distribution \mathcal{D} on $\mathcal{X} \times \mathbb{R}^C$ and a trained model $h(\mathbf{x}) = \beta^\top \phi(\mathbf{x})$, we define the information in a feature $f \in \mathcal{F}$ with respect to the c -th class component of $y \in \mathbb{R}^C$ as $\rho_{\mathcal{D}, \beta, c}(f) = \mathbb{E}_{(\mathbf{x}, y) \sim \mathcal{D}} [y_c \beta_c^\top f(\mathbf{x})]$, where $c \in \{1, \dots, C\}$ and β_c is c -th column of β .*

Corollary 3. *Let $(\lambda_i, \mathbf{u}_i)_{i=1,2,\dots}$ denote the eigenpairs of $\Sigma = \mathbb{E}_{\mathbf{x}} [\phi(\mathbf{x}) \phi(\mathbf{x})^\top]$. For any feature $f \in \mathcal{F}$ of the form $f = \tilde{\mathbf{U}} \tilde{\mathbf{U}}^\top \phi$, where $\tilde{\mathbf{U}} = [\mathbf{u}_1 \mathbf{u}_2 \dots \mathbf{u}_K]$ is a matrix of any K orthonormal eigenvectors of Σ , then information in feature f with respect to c -th component is given by*

$$\rho_{\mathcal{D}, \beta, c}(f) = \sum_{i=1}^K \lambda_i (\beta_c^\top \mathbf{u}_i)^2 = \sum_{i=1}^K s_c(\mathbf{u}_i).$$

Hence, the set of features selected in Algorithm 1 by sorting the robustness score $s_c(\mathbf{u}_i)$ also correspond to the eigenvectors with most information.

3.4 Connection to Neural Tangent Kernel features

Recently, Tsilivis and Kempe [34] defined features using NTK gram matrix and empirically observed that the features corresponding to the top spectrum of NTK are more robust and learned first during training. In the following, we define the NTK and NTK features and show its equivalence to our robust feature definition along with the proof that the robust NTK features correspond to the top of the spectrum. The NTK gram matrix $\Theta \in \mathbb{R}^{n \times n}$ is between all pairs of datapoints and the NTK between \mathbf{x}_i and \mathbf{x}_j for a network that outputs $f(\mathbf{w}, \mathbf{x})$ at data point $\mathbf{x} \in \mathbb{R}^d$ parameterized by $\mathbf{w} \in \mathbb{R}^p$ is defined by the gradient of the network with respect to \mathbf{w} as

$$\Theta(\mathbf{x}_i, \mathbf{x}_j) = \mathbb{E}_{\mathbf{w} \sim \mathcal{N}(0, \mathbf{I}_p)} [\nabla_{\mathbf{w}} f(\mathbf{w}, \mathbf{x}_i)^T \nabla_{\mathbf{w}} f(\mathbf{w}, \mathbf{x}_j)]. \quad (3)$$

For an extremely large width network, gradient descent optimization with least square loss is equivalent to kernel regression, the kernel being the NTK. Formally, for a data \mathbf{x} , the converged network output in the large width limit is $f(\mathbf{w}, \mathbf{x}) = \Theta(\mathbf{x}, \mathbf{X})^T \Theta(\mathbf{X}, \mathbf{X})^{-1} \mathbf{Y}$. Tsilivis and Kempe [34] define NTK features using the eigendecomposition of $\Theta(\mathbf{X}, \mathbf{X}) = \sum_{i=1}^n \lambda_i \mathbf{v}_i \mathbf{v}_i^T$ as

$$f(\mathbf{w}, \mathbf{x}) = \Theta(\mathbf{x}, \mathbf{X})^T \Theta(\mathbf{X}, \mathbf{X})^{-1} \mathbf{Y} = \sum_{i=1}^n \lambda_i^{-1} \Theta(\mathbf{x}, \mathbf{X})^T \mathbf{v}_i \mathbf{v}_i^T \mathbf{Y} := \sum_{i=1}^n f_i^{ker}(\mathbf{x}) \quad (4)$$

where $f_i^{ker}(\mathbf{x}) \in \mathbb{R}^C$ is the i -th NTK feature of \mathbf{x} . Note that f_i^{ker} is in accordance to our feature definition. We prove the empirical observation that the top spectrum-induced NTK features f_i^{ker} are more robust in the following proposition.

Proposition 4 (Robustness lies at the top.). *Let feature f_i^{ker} be Lipschitz continuous in gradient of NTK with respect to \mathbf{x} and an adversarial perturbation δ for input \mathbf{x} such that $\|\delta\|_p \leq \Delta$. Then, $\|f_i^{ker}(\mathbf{x} + \delta) - f_i^{ker}(\mathbf{x})\|_2 \leq \Theta(\frac{1}{\lambda_i})$.*

Proposition 4 shows that the NTK features corresponding to the higher eigenvalues are more robust to adversarial perturbations, and hence robustness lies at the top. This complements and strengthens the empirical observation in Tsilivis and Kempe [34]. The proof is provided in appendix.

Table 1: **Robust performance evaluation of RFI.** ℓ_∞ and ℓ_2 PGD attack on CIFAR-10 with Resnet-18. ℓ_∞ attack with step size $\epsilon/4$ and 40 iterations. ℓ_2 attack with size $\epsilon/5$ and 100 iterations.

Training	Clean		$\ell_\infty(\epsilon = \frac{8}{255})$		$\ell_2(\epsilon = 0.5)$	
	Method	+RFI	Method	+RFI	Method	+RFI
Standard	95.28	88.53	1.02	4.35	0.39	9.73
PGD [22]	83.53	83.22	42.20	43.29	54.61	55.03
IAT [21]	91.86	91.26	44.76	46.95	62.53	64.31
Robust CIFAR-10 [17]	78.69	78.75	1.30	7.01	9.63	11.00
C&W attack [6]	85.11	84.97	40.01	42.56	55.02	56.79

4 Experimental Results

We conduct extensive experiments to validate the performance of our algorithm, Robust Feature Inference, to different adversarial attacks on CIFAR-10 and CIFAR-100 [20] by integrating our method into several deep neural network models and different training procedures. We also compare our method to other adaptive test-time defenses. We first introduce the different evaluation methods for adversarial robustness that we use, network architectures, and other adaptive test-time defenses.

Evaluation methods. We evaluate our adaptive defense on different adversarial attacks namely, (a) Projected Gradient Descent (PGD) [22], a white box attack that perturbs the input within a small ℓ_p radius ϵ , so that it maximizes the loss of a model. We perform $\ell_\infty(\epsilon = 8/255)$ and $\ell_2(\epsilon = 0.5)$ PGD attack. We use the attack step size $\epsilon/4$ and 40 iterations for ℓ_∞ and $\epsilon/5$ and 100 iterations for ℓ_2 to have an overall high strength PGD attack. (b) Parameter-free attacks such as Auto PGD-Cross Entropy (APGD-CE) and Auto PGD-Difference Logit Ratios (APGD-DLR) [10] under $\ell_\infty(\epsilon = 8/255)$ threat model, that are extensions of PGD attack with no step size parameter and stronger than PGD. (c) RobustBench [11], a suite of white-box and black-box attacks including APGD-CE, APGD-DLR, Fast Adaptive Boundary Attack (FAB) [9], and Square Attacks [3]. RobustBench overcomes the limitations of auto-attack by flagging potential overestimation of robustness.

Benchmarking on SOTA methods. We evaluate our method on different settings: (a) Resnet-18 backbone with standard training and the popular adversarial training methods such as PGD [22], Interpolated Adversarial Training (IAT) [21], Carlini-Wagner (CW) loss [6] and also use Robust CIFAR-10 dataset created by Ilyas et al. [17]. (b) We select different state-of-the-art adversarially trained models [7, 13, 30, 38, 26] from RobustBench upon which at the test time we integrate RFI. These methods either use additional data [7, 38], informed adversarial prior [13] or early stopping based training [30] to improve the robustness of models. Carmon et al. [7] show that additional 500,000 unlabeled data improve robustness on CIFAR-10. Engstrom et al. [13] argue that the limitation of a network to represent input data in high-level features causes two semantically different images to have similar representation and propose training with an adversarial prior improves robustness. Rice et al. [30] suggest early stopping-based training to overcome this robust overfitting. Wang et al. [38] propose use of class-conditioned diffusion models to generate additional labeled data for adversarial training and observe state-of-the-art performance using additional 50 million synthetic images in training. We detail each training method in appendix.

Comparison to other adaptive test-time defenses. Recently, Croce et al. [12] provide an overview of 9 adaptive test-time defenses of which only four methods actually improve robustness and are competitive with the current state-of-the-art performances. We compare RFI with two out of the four methods: SODEF [19] and Anti-Adv [2]. The choice of SODEF and Anti-Adv is due to their relatively faster inference costs $2\times$ and $8\times$, respectively, and that they are representative of model adaptation and input modification strategies for adaptive test-time defenses, respectively.

4.1 Results and Discussion

Robust performance evaluation of RFI. We obtain clean and robust accuracy for standard and adversarially trained models before and after integrating RFI and setting K to the number of classes, that is, $K = 10$ and $K = 100$ for CIFAR-10 and CIFAR-100, respectively. The results for different training procedures on CIFAR-10 with ResNet-18 are presented in Table 1. We observe that our method improves the robust performance of adversarially trained models consistently, on an average

Table 2: **Effect of Adversary Strength.** Evaluation of RFI for ℓ_∞ and ℓ_2 PGD attack.

Method	ℓ_∞				ℓ_2		
	$\epsilon = \frac{2}{255}$	$\epsilon = \frac{4}{255}$	$\epsilon = \frac{12}{255}$	$\epsilon = \frac{16}{255}$	$\epsilon = 0.25$	$\epsilon = 0.75$	$\epsilon = 1.00$
PGD	74.60	64.02	23.34	11.66	71.34	40.91	28.25
PGD+RFI	74.99	64.91	24.32	12.55	71.48	41.95	29.24

by 2% and maximum by 6% for ℓ_∞ attack on Robust CIFAR-10 training. In table 3, we present the effectiveness of RFI on APGD-CE, APGD-DLR and RobustBench under ℓ_∞ ($\epsilon = 8/255$) threat model for different state-of-the-art methods. We observe that adding RFI at inference time improves the performance across all the methods. Importantly, RFI improves the robust performance (atleast marginally) for all the state-of-the-art methods, even though each one of them achieves robustness by incorporating very different strategies like additional data, early stopping or informed prior. This shows that strength and effectiveness of our method.

Effect of adversary strength. We study the effect of adversary strength on our method, RFI, by taking the adversarially trained ResNet-18 on CIFAR-10 using PGD ($\epsilon = 8/255$ for ℓ_∞ and $\epsilon = 0.5$ for ℓ_2) as the base model. Table 2 shows the evaluation of RFI with ℓ_∞ PGD attack for $\epsilon = \{2/255, 4/255, 12/255, 16/255\}$ and 40 iterations, and ℓ_2 attack for $\epsilon = \{0.25, 0.75, 1\}$ and 100 iterations. We observe that the underlying model augmented with RFI consistently improves over baseline across the perturbations of various strengths, especially by over 1% for adversary that is stronger than the base model ($\epsilon = \{12/255, 16/255\}$ for ℓ_∞ and $\epsilon = \{0.75, 1.00\}$ for ℓ_2).

Effect of parameter K . While we set K to be the number of classes, in Table 3 we also report the best performance of RFI by finding the optimal K using grid search. To study the effect of the parameter in detail, we vary K for the adversarial training methods on CIFAR-10 with ResNet-18 under ℓ_∞ ($\epsilon = 8/255$) threat model. Plot 1 of Figure 2 shows that the adversarial training methods (PGD, IAT and C&W) behave similarly in their accuracy profile as compared to standard training and Robust CIFAR-10 dataset. Moreover, the best performance is for $K = 10$ for all the robust training methods. The corresponding eigenvalue spectrum exhibits a knee drop after top-10 eigenvalues (plot 2), which motivates our choice of K as top-10 features for each class, equivalent to the number of classes. As a complementary explanation for our choice of K , neural collapse phenomenon observes that the penultimate feature of each class collapses to its mean during the terminal phase of training, that is, after the training error is almost zero [27]. This implies that there is principally only C number of feature vectors, one for each class, justifying our choice.

Top NTK features are indeed robust. To verify Proposition 4, we construct a sanity experiment using a simple 1-layer NN $f(\mathbf{x}) = \frac{1}{d}\mathbf{w}^T\mathbf{x}$ with parameters $\mathbf{w} \in \mathbb{R}^d$ initialized from $\mathcal{N}(\mathbf{0}, \mathbf{I}_d)$. Let the data dimension d be 100, the number of training samples n be 1000 and the data is sampled from a Gaussian $\mathcal{N}(\mathbf{0}, \Sigma)$ where the covariance Σ is a diagonal spiked matrix, that is, $\Sigma_{11} := 1 + \sqrt{d/n}$ and $\Sigma_{ii} := 1 \forall i \neq 1$. We then construct NTK features from the spectral decomposition of the exact NTK. Plot 3 of Figure 2 shows the norm of difference in the original, and adversarially perturbed NTK features with respect to the eigenvalues of the NTK spectrum for different perturbation strengths of $\Delta = \{0.01, 0.05, 0.1\}$. This validates our theory that the NTK features corresponding to the large eigenvalues are more robust and hence remain closer to the original feature even when perturbed.

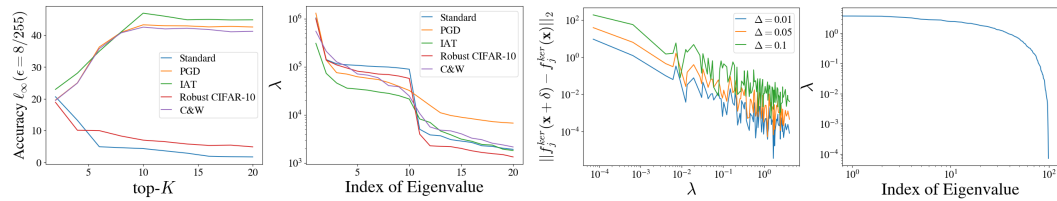


Figure 2: (Plots 1 and 2) Robust Accuracy for different K and the corresponding eigenvalue profile in ascending order of all the methods. (Plots 3 and 4) NTK feature robustness for λ and the corresponding eigenvalue profile in ascending order.

Table 3: **Robust performance evaluation of RFI on state-of-the-art methods.** We apply APGD-CE, APGD-DLR and RobustBench attacks on both CIFAR-10 and CIFAR-100. The inference time for RFI is $1\times$, whereas Anti-adv and SODEF are $8\times$ and $2\times$, respectively.

	Base Method	Adaptive Defense	Clean	APGD-CE	APGD-DLR	RobustBench
CIFAR-10	Carmon et al. [7] WideResNet-28-10	None	89.69	61.82	60.85	59.53
		Anti-adv [2]	89.69	61.81	60.89	58.70
		SODEF [19]	89.68	60.20	60.72	57.23
		RFI ($K = 10$)	89.60	62.38	61.58	60.72
		RFI (opt. $K = 20$)	89.60	62.45	61.60	61.02
	Engstrom et al. [13] ResNet-50	None	87.03	51.75	60.10	49.25
		Anti-adv [2]	87.00	51.62	59.95	49.20
		SODEF [19]	86.95	50.01	58.20	47.92
		RFI ($K = 10$)	87.01	51.86	61.84	50.75
		RFI (opt. $K = 15$)	87.03	51.94	61.90	50.98
	Rice et al. [30] WideResNet-34-10	None	85.34	50.12	56.80	53.42
		Anti-adv [2]	85.40	50.10	57.50	50.98
		SODEF [19]	85.10	50.60	56.50	50.09
		RFI ($K = 10$)	85.30	51.19	58.55	54.64
		RFI (opt. $K = 35$)	85.30	51.62	58.97	54.86
	Wang et al. [38] WideResNet-28-10	None	92.44	70.23	67.82	67.31
Anti-adv [2]		92.44	68.90	65.91	66.52	
SODEF [19]		92.01	67.53	65.08	64.20	
RFI ($K = 10$)		92.33	70.32	67.86	67.29	
RFI (opt. $K = 20$)		92.34	70.36	67.90	67.50	
Addepalli et al. [1] ResNet-18	None	65.45	33.49	28.55	27.67	
	Anti-adv [2]	65.38	30.92	26.61	26.01	
	SODEF [19]	65.23	29.37	26.90	26.53	
	RFI ($K = \text{opt. } K = 100$)	65.41	34.09	29.18	27.80	
	Pang et al. [26] WideResNet-28-10	None	63.66	35.29	31.71	31.08
Anti-adv [2]		63.41	32.50	30.32	30.10	
SODEF [19]		63.08	30.96	29.54	30.56	
RFI ($K = 100$)		63.01	36.03	31.95	31.29	
RFI (opt. $K = 115$)		63.10	36.07	31.95	31.91	
Rice et al. [30] WideResNet-34-10	None	53.83	20.83	20.46	18.95	
	Anti-adv [2]	53.83	20.78	20.06	18.97	
	SODEF [19]	53.83	18.50	19.20	16.92	
	RFI ($K = 100$)	53.70	21.10	20.98	19.23	
	RFI (opt. $K = 150$)	53.75	21.18	21.10	19.46	
Wang et al. [38] WideResNet-28-10	None	72.58	44.04	39.78	38.83	
	Anti-adv [2]	72.57	42.98	38.10	34.01	
	SODEF [19]	72.34	38.10	36.95	32.29	
	RFI ($K = 100$)	72.55	44.37	39.91	39.10	
	RFI (opt. $K = 115$)	72.55	44.51	39.96	39.13	

5 Conclusion

In this paper, we present a novel adaptive test-time defense that can be seamlessly integrated with any method at the time of deployment to improve the robustness of the underlying model. While the adaptive test-time defense as an approach offers promise to improve the robustness of models at the deployment stage, the general criticism of available methods is that they significantly increase the inference time of the underlying model. Our method, Robust Feature Inference (RFI), has no effect on the inference time of the underlying model which makes it a practical alternative for adaptive test-time defense. We also present a comprehensive theoretical justification for our approach describing the motivation behind retaining features in the top eigenspectrum of the feature covariance. In addition, we also show that these top features are more robust and informative, and validate our algorithm through extensive experiments. In conclusion, we propose the first theoretically guided adaptive test-time defense algorithm that has the same inference time as the base model with impressive

experimental results. Our findings contribute to the ongoing efforts to develop robust models that can resist adversarial examples and improve the security and reliability of DNNs.

6 Acknowledgment

The work of MS is supported through the German Research Foundation (Research Training Group GRK 2428). The authors would like to thank Siu Lun Chau (CISPA) for proof reading and providing feedback on the draft, and Julia Kempe (NYU) for helpful discussions.

References

- [1] Sravanti Addepalli, Samyak Jain, et al. Efficient and effective augmentation strategy for adversarial training. *Advances in Neural Information Processing Systems*, 35:1488–1501, 2022.
- [2] Motasem Alfarra, Juan C Pérez, Ali Thabet, Adel Bibi, Philip HS Torr, and Bernard Ghanem. Combating adversaries with anti-adversaries. In *Proceedings of the AAAI Conference on Artificial Intelligence*, volume 36, pages 5992–6000, 2022.
- [3] Maksym Andriushchenko, Francesco Croce, Nicolas Flammarion, and Matthias Hein. Square attack: a query-efficient black-box adversarial attack via random search. In *Computer Vision—ECCV 2020: 16th European Conference, Glasgow, UK, August 23–28, 2020, Proceedings, Part XXIII*, pages 484–501. Springer, 2020.
- [4] Sanjeev Arora, Simon S Du, Wei Hu, Zhiyuan Li, Russ R Salakhutdinov, and Ruosong Wang. On exact computation with an infinitely wide neural net. *Advances in neural information processing systems*, 32, 2019.
- [5] Anish Athalye, Logan Engstrom, Andrew Ilyas, and Kevin Kwok. Synthesizing robust adversarial examples. In *International conference on machine learning*, pages 284–293. PMLR, 2018.
- [6] Nicholas Carlini and David Wagner. Towards evaluating the robustness of neural networks. In *2017 IEEE Symposium on Security and Privacy (SP)*, pages 39–57. Ieee, 2017.
- [7] Yair Carmon, Aditi Raghunathan, Ludwig Schmidt, John C Duchi, and Percy S Liang. Unlabeled data improves adversarial robustness. *Advances in neural information processing systems*, 32, 2019.
- [8] Zhuotong Chen, Qianxiao Li, and Zheng Zhang. Towards robust neural networks via close-loop control. *arXiv preprint arXiv:2102.01862*, 2021.
- [9] Francesco Croce and Matthias Hein. Minimally distorted adversarial examples with a fast adaptive boundary attack. In *International Conference on Machine Learning*, pages 2196–2205. PMLR, 2020.
- [10] Francesco Croce and Matthias Hein. Reliable evaluation of adversarial robustness with an ensemble of diverse parameter-free attacks. In *International conference on machine learning*, pages 2206–2216. PMLR, 2020.
- [11] Francesco Croce, Maksym Andriushchenko, Vikash Sehwal, Edoardo DeBenedetti, Nicolas Flammarion, Mung Chiang, Prateek Mittal, and Matthias Hein. Robustbench: a standardized adversarial robustness benchmark. *arXiv preprint arXiv:2010.09670*, 2020.
- [12] Francesco Croce, Sven Gowal, Thomas Brunner, Evan Shelhamer, Matthias Hein, and Taylan Cemgil. Evaluating the adversarial robustness of adaptive test-time defenses. In *International Conference on Machine Learning*, pages 4421–4435. PMLR, 2022.
- [13] Logan Engstrom, Andrew Ilyas, Shibani Santurkar, Dimitris Tsipras, Brandon Tran, and Aleksander Madry. Adversarial robustness as a prior for learned representations. *arXiv preprint arXiv:1906.00945*, 2019.
- [14] Ian J Goodfellow, Jonathon Shlens, and Christian Szegedy. Explaining and harnessing adversarial examples. *arXiv preprint arXiv:1412.6572*, 2014.

- [15] Sven Gowal, Sylvestre-Alvise Rebuffi, Olivia Wiles, Florian Stimberg, Dan Andrei Calian, and Timothy Mann. Improving robustness using generated data. In *Advances in Neural Information Processing Systems*, 2021.
- [16] Duhun Hwang, Eunjung Lee, and Wonjong Rhee. Aid-purifier: A light auxiliary network for boosting adversarial defense. *Neurocomputing*, page 126251, 2023.
- [17] Andrew Ilyas, Shibani Santurkar, Dimitris Tsipras, Logan Engstrom, Brandon Tran, and Aleksander Madry. Adversarial examples are not bugs, they are features. *Advances in neural information processing systems*, 32, 2019.
- [18] Arthur Jacot, Franck Gabriel, and Clément Hongler. Neural tangent kernel: Convergence and generalization in neural networks. *Advances in neural information processing systems*, 31, 2018.
- [19] Qiyu Kang, Yang Song, Qinxu Ding, and Wee Peng Tay. Stable neural ode with lyapunov-stable equilibrium points for defending against adversarial attacks. *Advances in Neural Information Processing Systems*, 34:14925–14937, 2021.
- [20] Alex Krizhevsky, Geoffrey Hinton, et al. Learning multiple layers of features from tiny images. 2009.
- [21] Alex Lamb, Vikas Verma, Juho Kannala, and Yoshua Bengio. Interpolated adversarial training: Achieving robust neural networks without sacrificing too much accuracy. In *Proceedings of the 12th ACM Workshop on Artificial Intelligence and Security*, pages 95–103, 2019.
- [22] Aleksander Madry, Aleksandar Makelov, Ludwig Schmidt, Dimitris Tsipras, and Adrian Vladu. Towards deep learning models resistant to adversarial attacks. In *International Conference on Learning Representations (ICLR)*, 2018.
- [23] Chengzhi Mao, Mia Chiquier, Hao Wang, Junfeng Yang, and Carl Vondrick. Adversarial attacks are reversible with natural supervision. In *Proceedings of the IEEE/CVF International Conference on Computer Vision*, pages 661–671, 2021.
- [24] Gaurav Kumar Nayak, Ruchit Rawal, and Anirban Chakraborty. Dad: Data-free adversarial defense at test time. In *Proceedings of the IEEE/CVF Winter Conference on Applications of Computer Vision*, pages 3562–3571, 2022.
- [25] Weili Nie, Brandon Guo, Yujia Huang, Chaowei Xiao, Arash Vahdat, and Animashree Anandkumar. Diffusion models for adversarial purification. In *International Conference on Machine Learning*, pages 16805–16827. PMLR, 2022.
- [26] Tianyu Pang, Min Lin, Xiao Yang, Jun Zhu, and Shuicheng Yan. Robustness and accuracy could be reconcilable by (proper) definition. In *International Conference on Machine Learning*, pages 17258–17277. PMLR, 2022.
- [27] Vardan Pappayan, XY Han, and David L Donoho. Prevalence of neural collapse during the terminal phase of deep learning training. *Proceedings of the National Academy of Sciences*, 117(40):24652–24663, 2020.
- [28] Zhuang Qian, Shufei Zhang, Kaizhu Huang, Qiufeng Wang, Rui Zhang, and Xinpeng Yi. Improving model robustness with latent distribution locally and globally. *arXiv preprint arXiv:2107.04401*, 2021.
- [29] Sylvestre-Alvise Rebuffi, Sven Gowal, Dan A Calian, Florian Stimberg, Olivia Wiles, and Timothy Mann. Fixing data augmentation to improve adversarial robustness. *arXiv preprint arXiv:2103.01946*, 2021.
- [30] Leslie Rice, Eric Wong, and Zico Kolter. Overfitting in adversarially robust deep learning. In *International Conference on Machine Learning*, pages 8093–8104. PMLR, 2020.
- [31] Ali Shafahi, W Ronny Huang, Christoph Studer, Soheil Feizi, and Tom Goldstein. Are adversarial examples inevitable? In *International Conference on Learning Representations*, 2019.

- [32] Changhao Shi, Chester Holtz, and Gal Mishne. Online adversarial purification based on self-supervised learning. In *International Conference on Learning Representations*, 2021.
- [33] Christian Szegedy, Wojciech Zaremba, Ilya Sutskever, Joan Bruna, Dumitru Erhan, Ian Goodfellow, and Rob Fergus. Intriguing properties of neural networks. *arXiv preprint arXiv:1312.6199*, 2013.
- [34] Nikolaos Tsilivis and Julia Kempe. What can the neural tangent kernel tell us about adversarial robustness? *arXiv preprint arXiv:2210.05577*, 2022.
- [35] Dimitris Tsipras, Shibani Santurkar, Logan Engstrom, Alexander Turner, and Aleksander Madry. Robustness may be at odds with accuracy. *arXiv preprint arXiv:1805.12152*, 2018.
- [36] Dequan Wang, An Ju, Evan Shelhamer, David Wagner, and Trevor Darrell. Fighting gradients with gradients: Dynamic defenses against adversarial attacks. *arXiv preprint arXiv:2105.08714*, 2021.
- [37] Yu Wang, Wotao Yin, and Jinshan Zeng. Global convergence of admm in nonconvex nonsmooth optimization. *Journal of Scientific Computing*, 78:29–63, 2019.
- [38] Zekai Wang, Tianyu Pang, Chao Du, Min Lin, Weiwei Liu, and Shuicheng Yan. Better diffusion models further improve adversarial training. In *International Conference on Machine Learning*, 2023.
- [39] Boxi Wu, Heng Pan, Li Shen, Jindong Gu, Shuai Zhao, Zhifeng Li, Deng Cai, Xiaofei He, and Wei Liu. Attacking adversarial attacks as a defense. *arXiv preprint arXiv:2106.04938*, 2021.
- [40] Greg Yang. Scaling limits of wide neural networks with weight sharing: Gaussian process behavior, gradient independence, and neural tangent kernel derivation. *arXiv preprint arXiv:1902.04760*, 2019.
- [41] Hongyi Zhang, Moustapha Cisse, Yann N Dauphin, and David Lopez-Paz. mixup: Beyond empirical risk minimization. *arXiv preprint arXiv:1710.09412*, 2017.

A Proofs of the Main Results

In this section, we prove Theorem 1, and related results, Corollaries 2–3 and Remark 1.

A.1 Proof of Theorem 1

Proof. Recall that we assume $y = h(\mathbf{x}) + \epsilon = \boldsymbol{\beta}^\top \phi(\mathbf{x}) + \epsilon$, where $\epsilon \in \mathbb{R}^C$ has independent coordinates, each satisfying $\mathbb{E}[\epsilon_c] = 0$, $\mathbb{E}[\epsilon_c^2] \leq \sigma^2$ for all $c \in \{1, \dots, C\}$. The features for which we wish to compute robustness are of the form $f = \mathbf{M}\phi$ where \mathbf{M} is a linear map.

We are interested in robustness with respect to the c -th component, which is computed as

$$\begin{aligned} s_{\mathcal{D}, \beta, c}(f) &= \mathbb{E}_{(\mathbf{x}, y) \sim \mathcal{D}} \left[\inf_{\|\tilde{\mathbf{x}} - \mathbf{x}\|_2 \leq \Delta} y_c \boldsymbol{\beta}_c^\top f(\tilde{\mathbf{x}}) \right] \\ &= \mathbb{E}_{(\mathbf{x}, y) \sim \mathcal{D}} [y_c \boldsymbol{\beta}_c^\top f(\mathbf{x})] + \mathbb{E}_{(\mathbf{x}, y) \sim \mathcal{D}} \left[\inf_{\|\tilde{\mathbf{x}} - \mathbf{x}\|_2 \leq \Delta} y_c \boldsymbol{\beta}_c^\top (f(\tilde{\mathbf{x}}) - f(\mathbf{x})) \right]. \end{aligned} \quad (5)$$

We compute the first term exactly as

$$\begin{aligned} \mathbb{E}_{(\mathbf{x}, y) \sim \mathcal{D}} [y_c \boldsymbol{\beta}_c^\top f(\mathbf{x})] &= \mathbb{E}_{\mathbf{x}, \epsilon_c} [(\boldsymbol{\beta}_c^\top \phi(\mathbf{x}) + \epsilon_c) \boldsymbol{\beta}_c^\top f(\mathbf{x})] \\ &= \mathbb{E}_{\mathbf{x}} [\boldsymbol{\beta}_c^\top \phi(\mathbf{x}) \phi(\mathbf{x})^\top \mathbf{M} \boldsymbol{\beta}_c] && \text{since } \mathbb{E}[\epsilon_c] = 0 \\ &= \boldsymbol{\beta}_c^\top \Sigma \mathbf{M} \boldsymbol{\beta}_c, && \text{where } \Sigma = \mathbb{E}_{\mathbf{x}} [\phi(\mathbf{x}) \phi(\mathbf{x})^\top]. \end{aligned}$$

For the second term in (5), we aim to derive a lower bound. Observe that

$$\begin{aligned} y_c \boldsymbol{\beta}_c^\top (f(\tilde{\mathbf{x}}) - f(\mathbf{x})) &= y_c \boldsymbol{\beta}_c^\top \mathbf{M} (\phi(\tilde{\mathbf{x}}) - \phi(\mathbf{x})) \\ &\geq -|y_c| \cdot \|\boldsymbol{\beta}_c\|_{\mathcal{H}} \cdot \|\mathbf{M} (\phi(\tilde{\mathbf{x}}) - \phi(\mathbf{x}))\|_{\mathcal{H}} \\ &\geq -|y_c| \cdot \|\boldsymbol{\beta}_c\|_{\mathcal{H}} \cdot \|\mathbf{M}\|_{op} \cdot \|\phi(\tilde{\mathbf{x}}) - \phi(\mathbf{x})\|_{\mathcal{H}}. \end{aligned}$$

Using L -Lipschitzness of ϕ , we have $\|\phi(\tilde{\mathbf{x}}) - \phi(\mathbf{x})\|_{\mathcal{H}} \leq L \|\tilde{\mathbf{x}} - \mathbf{x}\|_2 \leq L\Delta$. Hence, the second term in (5) can be bounded from below as

$$\begin{aligned} \mathbb{E}_{(\mathbf{x}, y) \sim \mathcal{D}} \left[\inf_{\|\tilde{\mathbf{x}} - \mathbf{x}\|_2 \leq \Delta} y_c \boldsymbol{\beta}_c^\top (f(\tilde{\mathbf{x}}) - f(\mathbf{x})) \right] &= -\|\mathbf{M}\|_{op} \cdot \|\boldsymbol{\beta}_c\|_{\mathcal{H}} \cdot L\Delta \cdot \mathbb{E}_{\mathbf{x}, \epsilon_c} [|y_c|] \\ &\geq -\|\mathbf{M}\|_{op} \cdot \|\boldsymbol{\beta}_c\|_{\mathcal{H}} \cdot L\Delta \cdot \mathbb{E}_{\mathbf{x}, \epsilon_c} [|\boldsymbol{\beta}_c^\top \phi(\mathbf{x}) + \epsilon_c|] \end{aligned}$$

Finally, using Jensen's inequality, we can write

$$\mathbb{E}_{\mathbf{x}, \epsilon_c} [|\boldsymbol{\beta}_c^\top \phi(\mathbf{x}) + \epsilon_c|] \leq \sqrt{\mathbb{E}_{\mathbf{x}, \epsilon_c} [(\boldsymbol{\beta}_c^\top \phi(\mathbf{x}) + \epsilon_c)^2]} \leq \sqrt{\sigma^2 + \boldsymbol{\beta}_c^\top \Sigma \boldsymbol{\beta}_c}.$$

Combining the above computation leads to

$$s_{\mathcal{D}, \beta, c}(f) \geq \boldsymbol{\beta}_c^\top \Sigma \mathbf{M} \boldsymbol{\beta}_c - L\Delta \|\mathbf{M}\|_{op} \|\boldsymbol{\beta}_c\|_{\mathcal{H}} \sqrt{\sigma^2 + \boldsymbol{\beta}_c^\top \Sigma \boldsymbol{\beta}_c},$$

which proves Theorem 1. \square

A.2 Proof of Remark 1

Proof. The proof requires assumption of a Gaussian model, i.e., $\mathbf{x} \sim \mathcal{N}(0, \Sigma)$ and $\epsilon_c \sim \mathcal{N}(0, \sigma^2)$. Since the feature map is assumed to be linear, $\phi(\mathbf{x}) = \mathbf{x}$, it follows that $y_c = \boldsymbol{\beta}_c^\top \mathbf{x} + \epsilon_c$ is also Gaussian $y_c \sim \mathcal{N}(0, \sigma^2 + \boldsymbol{\beta}_c^\top \Sigma \boldsymbol{\beta}_c)$ and hence, $|y_c|$ is half-normal distributed.

Now recall that the first term in (5) can be computed exactly as $\boldsymbol{\beta}_c^\top \Sigma \mathbf{M} \boldsymbol{\beta}_c$. To compute the second term in (5), note that

$$\inf_{\|\tilde{\mathbf{x}} - \mathbf{x}\|_2 \leq \Delta} y_c \boldsymbol{\beta}_c^\top (f(\tilde{\mathbf{x}}) - f(\mathbf{x})) = \inf_{\|\tilde{\mathbf{x}} - \mathbf{x}\|_2 \leq \Delta} y_c \boldsymbol{\beta}_c^\top \mathbf{M} (\tilde{\mathbf{x}} - \mathbf{x})$$

and the infimum is achieved when the difference is aligned with $\mathbf{M}^\top \boldsymbol{\beta}_c$, that is, $\tilde{\mathbf{x}} = \mathbf{x} \pm \Delta \frac{\mathbf{M}^\top \boldsymbol{\beta}_c}{\|\mathbf{M}^\top \boldsymbol{\beta}_c\|_{\mathcal{H}}}$.

The sign depends on the sign of y_c , which leads to the second term in (5) compute to

$$\mathbb{E}_{(\mathbf{x}, y) \sim \mathcal{D}} \left[\inf_{\|\tilde{\mathbf{x}} - \mathbf{x}\|_2 \leq \Delta} y_c \boldsymbol{\beta}_c^\top (f(\tilde{\mathbf{x}}) - f(\mathbf{x})) \right] = -\mathbb{E}_{\mathbf{x}, \epsilon_c} [|y_c|] \cdot \Delta \cdot \|\mathbf{M}^\top \boldsymbol{\beta}_c\|_{\mathcal{H}}.$$

Since $|y_c|$ is half-normal, $\mathbb{E}[|y_c|] = \sqrt{2/\pi} \sqrt{\sigma^2 + \boldsymbol{\beta}_c^\top \Sigma \boldsymbol{\beta}_c}$, while $\|\mathbf{M}^\top \boldsymbol{\beta}_c\|_{\mathcal{H}} \leq \|\mathbf{M}\|_{op} \|\boldsymbol{\beta}_c\|_{\mathcal{H}}$, with the inequality being tight when $\boldsymbol{\beta}_c$ is the eigenvector of \mathbf{M} , corresponding to the largest eigenvalue. \square

A.3 Proofs of Corollary 2 and Corollary 3

Proof. In what follows, we restrict the linear map M as $M = \tilde{\mathbf{U}}\tilde{\mathbf{U}}^\top = \sum_{i=1}^K \mathbf{u}_i \mathbf{u}_i^\top$ where $\tilde{\mathbf{U}} = [\mathbf{u}_1, \dots, \mathbf{u}_K]$ is an orthonormal matrix of basis for a K -dimensional subspace. Since the operator norm $\|M\|_{op} = 1$ for projection matrix, the problem of finding the most robust subspace corresponds to maximising $\beta_c^\top \Sigma M \beta_c = \sum_{i=1}^K \beta_c^\top \Sigma \mathbf{u}_i \mathbf{u}_i^\top \beta_c$.

Note that if (λ, \mathbf{u}) is an eigenpair of Σ , then $\beta_c^\top \Sigma \mathbf{u} \mathbf{u}^\top \beta_c = \lambda (\beta_c^\top \mathbf{u})^2$. Hence, if we restrict the choice of $\mathbf{u}_1, \dots, \mathbf{u}_K$ to the eigenvectors of Σ , the optimal projection is obtained by choosing the K eigenvectors for which the robustness score $s_c(\mathbf{u}) = \lambda (\beta_c^\top \mathbf{u})^2$ are largest. So the claim of Corollary 2 holds only if the projections are restricted to eigenspaces of Σ . The claim of Corollary 3 follows along the same line as the information of the feature $f = M\phi$ can be computed as $\rho_{\mathcal{D}, \beta, c}(f) = \beta_c^\top \Sigma M \beta_c$. For the case of $M = \tilde{\mathbf{U}}\tilde{\mathbf{U}}^\top$ where $\tilde{\mathbf{U}}$ is matrix of K eigenvectors of Σ , we have $\rho_{\mathcal{D}, \beta, c}(f) = \sum_{i=1}^K \lambda_i (\beta_c^\top \mathbf{u}_i)^2$. Hence, if the search is restricted to eigenspaces of Σ , the most robust features also correspond to the most informative ones. \square

Robust and informative features over all possible K -dimensional subspaces. If we consider $M = \tilde{\mathbf{U}}\tilde{\mathbf{U}}^\top$ for any $\tilde{\mathbf{U}} = [\mathbf{u}_1, \dots, \mathbf{u}_K]$ with orthonormal columns, as assumed in Corollary 2, then

$$\beta_c^\top \Sigma M \beta_c = \sum_{i=1}^K \beta_c^\top \Sigma \mathbf{u}_i \mathbf{u}_i^\top \beta_c = \text{Trace} \left(\tilde{\mathbf{U}} \beta_c \beta_c^\top \Sigma \tilde{\mathbf{U}}^\top \right) = \text{Trace} \left(\tilde{\mathbf{U}} \Sigma \beta_c \beta_c^\top \tilde{\mathbf{U}}^\top \right),$$

where the last equality follows from taking transpose. Hence, the resulting maximisation problem can be written as

$$\max_{\tilde{\mathbf{U}}} \beta_c^\top \Sigma M \beta_c \equiv \max_{\tilde{\mathbf{U}}} \text{Trace} \left(\tilde{\mathbf{U}} \beta_c \beta_c^\top \Sigma \tilde{\mathbf{U}}^\top \right) \equiv \max_{\tilde{\mathbf{U}}} \text{Trace} \left(\tilde{\mathbf{U}} \mathbf{B}_c \tilde{\mathbf{U}}^\top \right), \quad (6)$$

where $\mathbf{B}_c = \frac{1}{2} (\beta_c \beta_c^\top \Sigma + \Sigma \beta_c \beta_c^\top)$. The above trace maximisation problem corresponds to finding the K dominant eigenvectors of the matrix \mathbf{B}_c . This leads to an alternative to Algorithm 1 for finding robust projections for the test-time defense. The approach comprises of computing the dominant eigenvectors $\tilde{\mathbf{U}}_c$ of the matrix \mathbf{B}_c for every class component $c \in \{1, \dots, C\}$ and defining the robust output as $\tilde{h}(\mathbf{x}) = [\beta_1^\top \tilde{\mathbf{U}}_1 \tilde{\mathbf{U}}_1^\top \phi(\mathbf{x}), \dots, \beta_C^\top \tilde{\mathbf{U}}_C \tilde{\mathbf{U}}_C^\top \phi(\mathbf{x})]$. The approach would result in theoretically more robust projections, but suffers computationally since it requires $(C + 1)$ eigendecompositions instead of only one eigendecomposition in Algorithm 1. Hence, it has $O(C)$ more one-time computation than Algorithm 1, but with identical inference time. The conclusion of Corollary 3 that the most robust features, obtained from the maximisation in (6), are also the most informative features still holds in this case.

A.4 Proof of Proposition 4

Proof. Suppose that the NTK feature f_i^{ker} is L -Lipschitz continuous in gradient of NTK with respect to \mathbf{x} . Then, we have

$$\|\nabla_{\mathbf{x}} \Theta(\mathbf{x} + \delta, \mathbf{X}) - \nabla_{\mathbf{x}} \Theta(\mathbf{x}, \mathbf{X})\|_2 \leq L \|\delta\|_2. \quad (7)$$

Recall that we can write the i -th NTK feature as $f_i^{ker}(\mathbf{x}) := \lambda_i^{-1} \Theta(\mathbf{x}, \mathbf{X})^\top \mathbf{v}_i \mathbf{v}_i^\top \mathbf{Y}$. Bounding $\|f_i^{ker}(\mathbf{x} + \delta) - f_i^{ker}(\mathbf{x})\|_2$ by Taylor's expansion and applying (7) yield

$$\begin{aligned} \|f_i^{ker}(\mathbf{x} + \delta) - f_i^{ker}(\mathbf{x})\|_2 &\stackrel{(a)}{=} \left\| \lambda_i^{-1} \delta^\top \nabla_{\mathbf{x}} \Theta(\mathbf{x}, \mathbf{X}) \mathbf{v}_i \mathbf{v}_i^\top \mathbf{Y} + \lambda_i^{-1} \mathbf{R} \mathbf{v}_i \mathbf{v}_i^\top \mathbf{Y} \right\|_2 \quad \mathbf{R} : \text{remainder} \\ &\stackrel{(b)}{\leq} \left\| \lambda_i^{-1} \delta^\top \nabla_{\mathbf{x}} \Theta(\mathbf{x}, \mathbf{X}) \mathbf{v}_i \mathbf{v}_i^\top \mathbf{Y} + \frac{\lambda_i^{-1} L}{2} \|\delta\|_2 \mathbf{v}_i \mathbf{v}_i^\top \mathbf{Y} \right\|_2 \quad \text{from (7)} \\ &\leq \lambda_i^{-1} \left\| \left(\delta^\top \nabla_{\mathbf{x}} \Theta(\mathbf{x}, \mathbf{X}) + \frac{L}{2} \|\delta\|_2 \right) \mathbf{v}_i \mathbf{v}_i^\top \mathbf{Y} \right\|_2 = \Theta \left(\frac{1}{\lambda_i} \right) \end{aligned}$$

where (a) follows from the Taylor's expansion of $f_i^{ker}(\mathbf{x} + \delta)$ where \mathbf{R} is the remainder terms and (b) follows from (7), i.e., $\mathbf{R} \leq (L/2) \|\delta\|_2$. \square

B Experimental Details

B.1 Details of Benchmarking baseline SOTA methods

We perform Bench-marking of our adaptive test time defense on multiple SOTA methods that are used achieving adversarial robustness in the model. For our analysis of proposed adaptive test time defense on CIFAR-10 in table 1 we used PGD [22], Interpolated Adversarial Training [21], Carlini-Wagner Loss [6] and Robust CIFAR-10 [17] to adversarially train the baseline model. In general for PGD, IAT and CW Attack the adversarial training works as generating an adversarial example using the underlying attack and the objective to minimize loss on these adversarial examples. PGD attack uses gradient descent to iteratively maximize the classification loss with respect to the input while projecting the perturbed example into the norm ball defined for the attack. IAT uses a joint objective that minimizes the classification loss of perturbed examples generated from PGD or any other attack along with classification loss on clean data with MixUP [41]. We use Robust CIFAR-10 proposed in [17], although is not an adversarial training method but rather the final dataset from a procedure to only retain robust features in the dataset. Ilyas et al. [17] disentangle the robust and non robust features by creating a one to one mapping of an input to its robustified image. From an adversarially pretrained backbone (ResNet-18 using PGD ℓ_2 -norm and $\epsilon = 0.25$) linear layer features are extracted for the natural image and also from a noise input. Then by minimizing the distance between these two representations in the input space over the noise, a image which only retains robust features of the original input is obtained.

For training using all these baseline adversarial training methods we set the batch size as 128. We use SGD with momentum as the optimizer where we set the momentum to be 0.1, we also set the weight decay to 0.0002. We run our training for 200 epochs and set the learning rate schedule as starting with 0.1 for first 100 epochs and then we reduce the learning rate by 90 percent every 50 epochs.

For table 3 we benchmark our adaptive test time defense on multiple recent state-of-the-art methods for both CIFAR-10 and CIFAR100 datasets. For all our baseline methods we obtain the model weights from RobustBench [10]. We then update the weights of all underlying models in their last linear layer using our adaptive test time defense method and benchmark the updated model with RobustBench. We provide our implementation of benchmarking experiments along with supplementary material.